Regional correlations for estimating seismic amplification. Implications for lossmassessment In SW Iberia (https://doi.org/10.1016/j.soildyn.2019.105993).
Autores: Luis Fazendeiro Sá, Antonio Morales-Esteban, Percy Durand Neyra.
Revista: Soil Dynamics and Earthquake Engineering, 2020, 130,105993.

DOI: https://doi.org/10.1016/j.soildyn.2019.105993

Regional correlations for estimating seismic amplification. Implications for loss assessment in SW Iberia.

[1]Luis Fazendeiro Sá, [23]*Antonio Morales-Esteban, [23]Percy Durand Neyra

[1] Emergency Planning National Department, Portuguese National Authority for Civil Protection. luis.sa@prociv.pt

[2] Department of Building Structures and Geotechnical Engineering. University of Seville. Av. Reina Mercedes 2, 41012 (Spain). ame@us.es / percy@us.es

[3] University Institute of Architecture and Construction Sciences, University of Seville (Spain)

Abstract

Most earthquake-related losses are enhanced by soil amplification phenomena, especially in areas where high vulnerability assets coexist. These mechanisms are frequently inferred from empirical formulas. These procedures are based on the average shear-wave velocity to 30 m depth (V_{s30}) as a proxy for amplification events. However, past analysis of spatial relationships between the V_{s30} and nonlinear soil behaviour has frequently resulted in poor correlations, affecting all onward analysis. In this research, these relationships are further analysed using an Earthquake Loss Estimation Software. In this framework, the Algarve region and associated ground motion have been depicted based on a certified seismic catalogue. This region has a moderate seismic hazard but possesses a complex geology and dissimilar seismogenic sources. The source data for this research has been V_{s30} data collected from geologic surveys made for the region in 2010 in the framework of the Study of Seismic Risk and Tsunamis in Algarve (ERSTA) coordinated by the Portuguese Civil Protection. Other data collected has been the V_{s30} topography compiled by the USGS and geologic information available by the OneGeology collaborative project. The goal of this research is to identify inaccuracies that potentially occur in estimating the site effects by different approaches. In this framework three amplification factors based on different sources - V_{s30} field-data, V_{s30} using slope as proxy and V_{s30} using geology as proxy – have been tested. The results have shown a good correlation between V_{s30}-field-data and geologic based V_{s30} and a minor correlation between the former and slope based V_{s30}. However, regarding the seismic losses -

building damage and human losses - the final results show similar values for all three amplification factors analysed.

1. Introduction

Earthquakes, through their overwhelming consequences, are a critical threat that society faces. The increase of the seismic intensities in soft sediments is a key factor accountable for the amplification of earthquake motions. A precise characterisation of the behaviour of the ground under static and dynamic loads is essential in terms of a correct structuring and construction safety (García-Jerez *et al.*, 2008). The shear-wave (S-wave) velocity (V_s) is a paramount parameter in seismic engineering. Since soil density is relatively constant with depth, the V_s value can be used to represent the site conditions. In fact, in an ordinary approach it can be assumed that the amplification (A_k) is usually proportional to (Aki and Richards, 1981):

$$A_k = 1/\sqrt{V_s \cdot \rho} \quad \textbf{(1)}$$

where V_s is the S-wave velocity and ρ is the density of the soil.

In recent years, the notion "average V_s information for the first 30m of the sub-surface (V_{s30}) is sufficient to characterize the ground" and has been broadly accepted in terms of engineering analysis (Poormirzaee and Moghadam, 2014). However, it is manifest that the V_{s30} cannot properly represent the ground response in all cases (Ozcep *et al.*, 2013). The V_{s30} is a simple metric that can be obtained at a relatively low cost compared to more detailed descriptions of the site characteristics. Moreover, it is correlated with site amplifications (Boore *et al.*, 1993). The V_{s30} is calculated by the expression defined in the International Building Code - IBC 2000 (Paz and Leigh, 2004):

$$V_{s30} = 30/\sum_{i=1}^{N}(h_i/v_i) \quad \textbf{(2)}$$

where h_i and v_i are, respectively, the thickness and the S-wave velocity of the i_{th} layer, in a total of N in the top 30 m.

Despite being classified only as a proxy for site amplification (Castellaro *et al.*, 2008), the V_{s30} is commonly used. Moreover, several national design codes, following the requirements of the Eurocode 8 (EC8) (EN1998-1, 2004), have adopted the V_{s30} as a standard to characterise the site conditions. However, assuming that V_{s30} values from California can be used elsewhere without modification is misleading (Wald and Mori, 2000). This shortcoming has resulted in untrustworthy amplification factors for other locations (Rodríguez-Marek *et al.*, 2001). This is due to the fact that the amplitude of seismic waves, within a layered media, changes during movement according to the different layers' impedances (Le Pense *et al.*, 2011). However, recent studies have proposed several alternatives or supplemental parameters to VS30.In fact, new site-condition proxies like depth to seismic bedrock with V_s = 800m/s (H800) or fundamental period (f_0) have been proposed by several authors like (Castellaro *et al.*, 2008) or (Pitilakis *et al.*, 2013). In this framework (Bisch P., 2018) concluded that also based on "real data", is evident that the depth of the soil where Vs = 800 m/s is important (H800). That conclusion explains why the Eurocode 8 new version is adopting this new parameter to account for possible site amplification (Pitilakis, 2015). Nevertheless, (Derras *et al.* 2016), analysed the performance of various site-condition proxies in reducing ground-motion aleatory variability and concluded that in certain conditions - short periods events like PGA - Vs30 is still the best of single proxies. In fact, although (Kotha *et al*., 2018) cited limitations on the usage of Vs30 parameter, (Rahman *et al.*, 2016) concluded that Vs30 captures the general amplification for soil with a shear velocity range limit of 600-800 m/sec, concluding that caution must be applied in extrapolating Vs30 scaling to rock or rock-like sites (EC8 soil class A).

Although the limitations above cited are of relevant nature, the authors chose to uphold Vs30 as proxy for analysing site effects phenomena. That decision was established based on few keys aspects:

a) Almost all high vulnerable areas of Algarve are located in softer soils (Vs30<600 m/s);
b) The field data collect and process by (Silva *et al.*, 2007) didn't include variables like H800 or F_0;
c) Vs30 is used for characterizing site-conditions in numerous ground motion prediction equations, and for modeling ground motion amplification in both seismic hazard and instrumental intensity maps (Vilanova *et al.*, 2018);
d) In regional studies, where local field data is not easily obtained, a simplified methodology is necessary. (Vilanova *et al.*, 2018) defined that although the detailed study of site-effects is

essential for site-specific, regional assessments must unescapably depend on simplified approaches;

e) This notion is enhanced by the geographic scale of this research. In fact, this research lies at a sub-national level – Algarve is a Territorial Unit Class 2 or NUT2 (Eurostat, 2019);

f) No alternative thus far has been suggested for a single, effective, continuous parameter that can work well for a large global dataset, and that Vs30 will probably continue to dominate GMPE site classification for the near future (Kamal *et al.*, 2016).

Throughout the rest of this introduction, one will begin to see the overall area that has been studied. Its seismicity and geology will be briefly described. Then, the V_{s30} variables used in this research will be described, followed by an overview of the goals of this paper.

1.1 Seismicity and geology of the Algarve

SW Iberia in general is an area where the existence of the site effect phenomenon is known. However, the time interval of the occurrence of a significant earthquake – as M_w7.9 in 1969 (Gutscher *et al.*, 2006) - makes real data be of low extent. Therefore, numerical methods or empirical approaches must be used. The latter are based on data that rely on relationships from earthquake motions elsewhere and surface geology (Borges *et al.*, 2015). The seismic activity of SW Iberia is moderate and earthquakes of M_w<5 are probable (Amaro-Mellado *et al.*, 2017b). The recurrence interval of events with a large magnitude (M_w>8) is long (Amaro-Mellado *et al.*, 2017a). Historical earthquakes have affected major cities, causing human and physical damage. Examples are the cases of the 1531 and 1755 Earthquakes (Sá *et al.*, 2018) (Chester, 2001). The results by (Peláez Montilla *et al.*, 2002) showed that the hazard of many cities of the SW Iberia is almost entirely due to the local seismicity.

The standard values for the Peak Ground Acceleration (PGA) have been obtained from (Crespo *et al.*, 2013). In Algarve, for a 0.1s period, the PGA of 0.30g has a return period of 475 years -10% chance of exceedance in 50 years- and the PGA of 0.75g has a return period of 2475 years -2% chance of exceedance in 50 years - Figure 1.

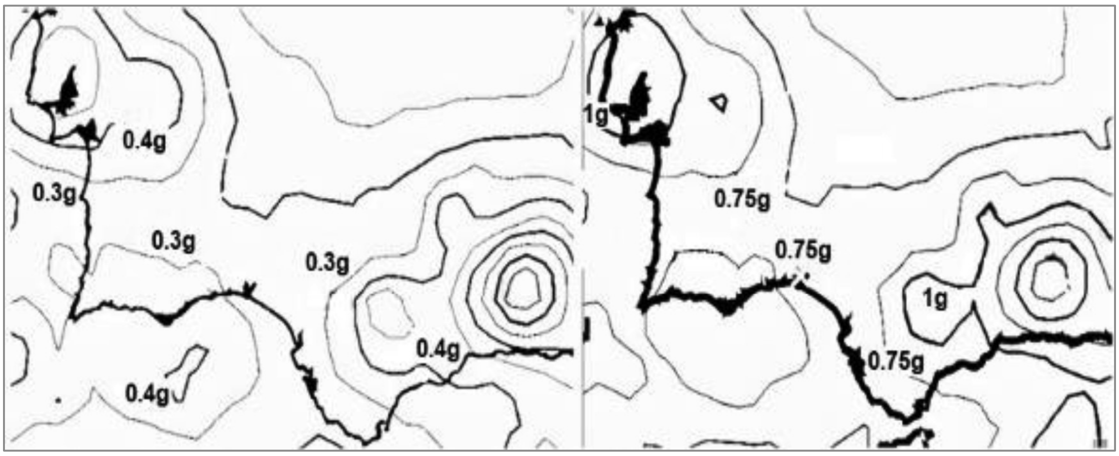

Figure 1. PGA (0.1s) for 475 (left) and 2475 (right) years of return period, adapted from (Crespo *et al.*, 2013)**.**

Regarding the geology of the area, in the NW Algarve, the Paleozoic basement is interloped at Monchique by an igneous chain of the Upper Cretaceous age. In the south, Mesozoic and Cenozoic rocks can be found in two sedimentary basins. The Cenozoic deposits include fossiliferous biocalcarenites of the Lower-Middle Miocene age, overlaid by sandstones of the Upper Miocene age (Pais *et al.*, 2000). The uppermost Miocene deposits are the Mem Martins spongoliths and the Cacela formation (Antunes and Pais, 1993) (Brachert *et al.*, 2003). There are sands and sandstones of the Pliocene-Upper Miocene age at the centre of the Algarve (Antunes *et al.*, 2000). Pliocene to Pleistocene reddish sands and conglomerates overly the Miocene sediments (Manuppella, 1992) (Moura and Boski, 1999). Plio-Quaternary deposits eventually reach 30 m, whereas the underlying Miocene formations may be of 200 meters (Geirnaert *et al.*, 1982). To the south there are sediments of the Tertiary-Quaternary age (Leyva and Ramírez, 1979) (Salazar Rincón, 2006), associated with fluvial drainage.

Regarding the paleography, the Cenozoic sedimentation of the Algarve is continued in the Guadalquivir basin. The Miocene *Lagos-Portimão* formation is formed by packstones and rudstone (Dabrio *et al.*, 2008). The Cacela formation consists of sediments formed by earlier lagoons. Finally, there are several levels of terraces and alluvium formations inserted into the local river basins (Cunha *et al.*, 2009).

1.2 V_{s30} ~~field~~ measurements

The evaluation of the V_{s30} in the Algarve has been the goal of recent projects: SCENE (Narciso *et al.*, 2013); ERSTA[1] (Autoridade Nacional de Protecção Civil - ANPC, 2010); and CAPSA (Carvalho *et al.*, 2008). Due to the focus of ERSTA project on the Algarve region, their values have been used as the main data source for this research. In fact, in ERSTA scope, a geological and geotechnical survey was carried out in the year 2007. For this analysis 280 ground tests data were evaluated, enabling the gathering of relevant geotechnical information with in-situ penetration resistance SPT tests regarding the establishment of a Vs profile. More information on the ERSTA survey and the usage of the collected data please refer to (Silva *et al.*, 2007) and (ANPC, 2010)

Besides field data, V_{s30} proxies were also considered for this research. In this context, past uses of (Wills and Clahan, 2006) geological method and (Wald and Allen, 2007) topographic slope method produced good estimates of V_{s30} for some geological classes while produced dissimilar results for others (Vilanova *et al.*, 2018. In the Algarve area (Narciso *et al.*, 2013), that also uses ERSTA Vs30 field values, stated that "*while some geological units display very consistent values of V_{s30}, others are characterized by a broad dispersion*". (Narciso *et al.*, 2013) concluded that "*It seems to be particularly difficult to evaluate and systematize the V_{s30} values obtained for Miocene formations*". This is poignant in Algarve where Miocene formations coexist with areas of high population density, especially near the shoreline, as can be observed in Figure 2.

[1] ERSTA is "*The Study of Seismic Risk and Tsunami in Algarve*" developed by the Portuguese Civil Protection.

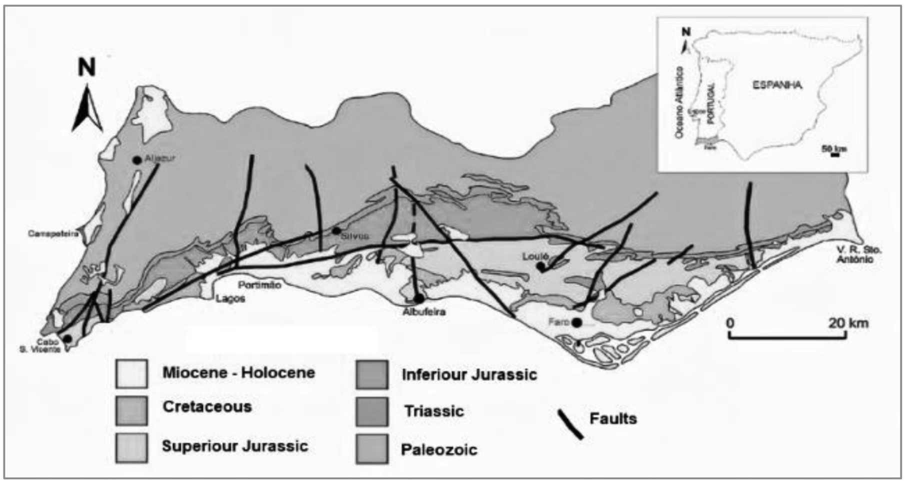

Figure 2. Active faults and Geologic time Period of Algarve, adapted from (Dias and Cabral, 2002)**.**

In fact, Earthquake Loss Estimation Software (ELES) typically uses an algorithm for amplifications predictions based on the V_{s30} values combined with the procedure proposed by (Park and Hashash, 2004) and (Borcherdt *et al.*, 1991). This procedure estimates the site-dependent response spectra and subsequent amplifications, but does not examine the use of different V_{s30} estimations - as amplification proxy - for predicting seismic losses.

1.3 Research goals

In this framework, the goal of this research is to assess the responsiveness of loss assessment, by using different sources of V_{s30} values as proxy to estimate nonlinear soil effects.

2. Method

This section is structured as follows. First, the determination of the ground motion at the bedrock is explained. Second, the method to estimate the site effects is presented. To do so, an amplification factor between the surface and the bedrock is proposed. Finally, the method to estimate the intensity felt is shown. It is important to enhance that the arguments presented in this paper will be limited to the linear site-response and its correlation with Vs30. The non-linear dependence on Vs30 or other site classification indices are a more complex topic which is beyond the scope of this paper.

2.1 Determination of the bedrock ground motion

The assumptions on choosing the model for ground motion were based in:

- ✓ ~~Stochastic methods have been used for modelling the ground motion (Boore, 1983) (Boore and Atkinson, 1987);~~
- ✓ The absence of recent relevant earthquakes in the study region requires the use of synthetic models for attenuation and seismic studies (Silva *et al.*, 2015).
- ✓ The last strong earthquake felt in Algarve was about 50 years ago, in 1969, (Mw 7.8). As such, we can accept that instrumental strong-motion data for Algarve is limited. Therefore, most of the seismic hazard studies are to be built upon historical data and macroseismic information, which characteristically has a larger uncertainty.
- ✓ The "no new relevant observations" condition in practice prevents new research to be developed like the one presented by (Gaudio *et. al*., 2019) that relies on peak ground motion observations to recommend new GMPEs for Italy, where a large amount of new and relevant observations is available.

For overrun the listed issues, the probabilistic seismic-hazard map by (Vilanova and Fonseca, 2007) has been selected from among the models that fulfil the above conditions. This model, which was not yet superseded by an enhanced proposal, is an application that addresses in detail the Portuguese tectonic characteristics, considering a large spectrum of aleatory uncertainties and takes into attention several previous studies in its creation.

As such, area sources were employed to define the seismicity according to two zonations: one comprising eleven area sources drawn based on the isoseismal maps from historical events *(Silva et al.*, 2015). (Vilanova and Fonseca, 2007) considered mainland Portugal as a stable continental region, although the offshore areas of south and southern Spain have been studied as active shallow crustal regions. Three GMPEs have been proposed to assess the rock level ground motion in this model: (Ambraseys *et al.*, 1996), (Toro *et al.*, 1997) and (Atkinson and Boore, 1997). These GMPEs have been combined in a logic tree approach (Annaka *et al.,* 2007) with a weighted arithmetic mean of respectively 20%, 40% and 40% as proposed by (Vilanova and Fonseca, 2007). All the GMPEs selected have a similar structure as enunciated by (Toro, 2002), which is described in Equation (3):

$$\ln PGA = C_1 + C_2(M-6) + C_3(M-6)^2 - C_4R_m - (C_5 - C_4)max\left(\log\left(\frac{R_m}{100}\right), 0\right) - C_6R_m + \gamma_a + \gamma_b \quad \textbf{(3)}$$

where R_m is $(R^2+C_7)^{1/2}$, R is the horizontal distance, C_1 to C_7 are the regional variables, M is the moment magnitude, γ_a is the epistemic uncertainty and γ_b is an aleatory uncertainty.

To run the model analysis, two ground motion scenarios from the catalogue built by (Vilanova and Fonseca, 2007) for SW Iberia have been selected:

I. Inland event - (Lat 37.10; Long -8.00) M_w5.5, 1856 Loulé earthquake (Carvalho *et al.*, 2012).
II. Onshore event - (Lat 36.20; Long -10.60) M_w7.8, 1969 Gorringe earthquake (Grandin *et al.*, 2007).

In addition to (Vilanova and Fonseca, 2007) proposal, newer models by (Atkinson and Boore 2006), (Douglas *et al.* 2006) and (Atkinson, 2008) were also considered as potentially applicable by (Silva et. al., 2015). However, it is relevant to recognize that such models were compiled to provide the best fit for Europe in general and thus, they not fulfil the requirements for the specific region of Algarve. The active shallow crustal region (ASCR) near Algarve is considerably different from other ASCR in Europe, due to a very low attenuation which is typically observed in stable crustal regions, rather than a high to very high attenuation, frequently reported in other Iberian regions of the same regime, like the Pyrenees area (Casado *et al.* 2000) (Vilanova and Fonseca 2007). This behavior was verified by Vilanova et al. (2012) and Silva et al. (2015). Both works analyzed the performance of a set of ground motion prediction equations that were evaluated against instrumental and historical data from Western Iberia. They concluded that new attenuation models developed for European ASCR performed poorly for the Algarve area - especially in offshore events- noticeably underestimating the ground motion.

2.2 Determination of the site effects

By using Vs30 as proxy for estimating site effects, other assumptions were established. The soil amplification factor (A_k) has been assumed as the peak value of spectrum ratio between ground surface and the bedrock. The PGA values obtained for both scenarios (Loulé/Gorringe) by the (Vilanova and Fonseca, 2007) model have been converted into Pseudo Spectral Acceleration (PSA). To do so, the equation proposed in the EC8 (EN1998-1, 2004) and reaffirmed by (Booth, 2007) has been used:

$$PGA = \frac{peak\ 5\%\ damped\ PSA}{2.5}\text{, for a time period of one second} \quad \textbf{(4)}$$

For the calculation of A_k, different approaches have been implemented (Figure 3):

i. The use of empirical equations that relate the amplification factor to V_{s30};
ii. The usage of remote sensing data to infer the V_{s30} and its relation with the amplification factor;

The analytical method for modelling site response used in this research is based on a 1D soil layer model, by assuming the following simplifications:

i. The movement of the shear waves is vertical to the soil layers;
ii. The boundaries of the layers are horizontal;
iii. The surface of the soil and the bedrock are crosswise infinite;
iv. Soils are stiffer at larger depths and softer closer to the surface;
v. Each layer is considered a homogeneous material with the same properties in S and P waves (Vs and Vp), and density;
vi. The thickness of each layer tends to be smaller at the top, and increases with depth;
vii. There is a linear site response;
viii. Presence of linear elastic conditions;
ix. Under the deformable soil layer was considered a rigid reflecting bedrock.

As above noted, based on this method, the amplification frequency is dependent on the geometry and soil properties (V_s). That is, site response is the effect of shallow soil layers on the seismic surface ground motion. In most site response analyses, only horizontal ground motion is considered, as it is the dominant motion component responsible for structural damage (Pruiksma, 2016). In fact, the 1D wave propagation assumption implies that the medium consists of laterally constant layers overlying a half-space, wave fronts are planar, and only the horizontally polarized component of the shear wave (SH) is modelled.

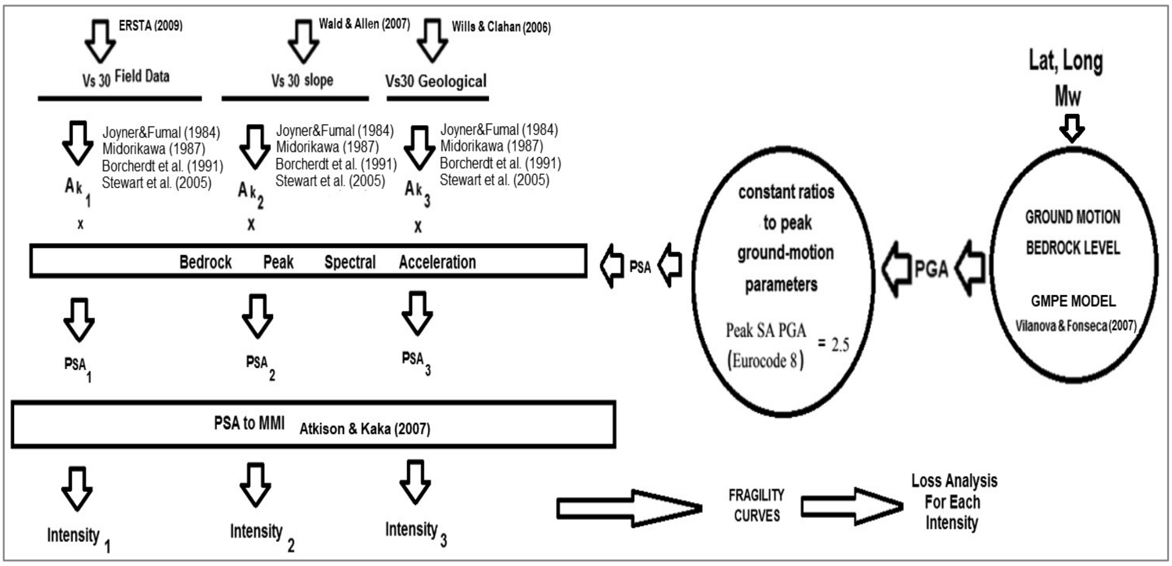

Figure 3. Flow diagram used to obtain the amplification estimation.

The methodology proposed in this research evaluates the amplification by normalising the spectra of the motions recorded to the reference acceleration spectrum obtained from the GMPEs. It is a non-reference site approach since it does not depend on the availability of an adequate reference site (Field and Jacob, 1995). Analogously, non-reference site approaches have been used among others by (Sokolov *et al.*, 2000).

3. Calculation

3.1 Determination of V_{s30}

It has been mentioned before that the V_{s30} is a proxy variable used to determine the nonlinear soil effect due to a seismic action. It is also known that both the current version of EC8 (EN1998-1, 2004) for Europe and the NEHRP Recommended Seismic Previsions (FEMA, 2015) for the USA use the V_{s30} to classify the soil type for earthquake engineering design. Ordinarily, this variable is obtained from the following methods (Silva *et al.*, 2015):

- ✓ Soil geotechnical analysis – V_{s30}-field-data (as a proxy for A_{k1}). The following sources have been used: local geotechnical data from earlier works, also obtained from the drilling of underground wells. The geoprocessing tool "Zonal Analysis" (Murayama and Estoque, 2011) has been used in distributing V_{s30} by sub-census block. This enabled the creation of the V_{s30} distribution map - Figure 4 - considering the EC8 classification (EN1998-1, 2004).

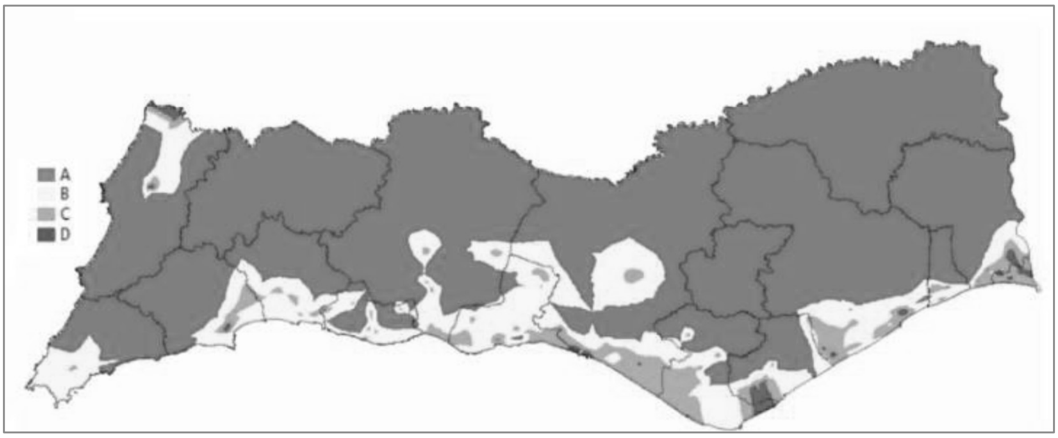

Figure 4. EC8 soil class map - ERSTA V_{s30} as source

- ✓ Topography generated maps - V_{s30}-slope (as proxy for A_{k2}). For this approach, a Digital Elevation Model (DEM) based on remote sensing data is proposed. (Wald and Allen, 2007) developed the possibility of using a USGS database of DEMs. (Wald and Allen, 2007) used the proxy of ground slope gradient at 30 arcsec resolution to estimate the V_{s30}. The match between the V_{s30} and the slope range has been obtained according to (Silva *et al.*, 2015). A GIS has been used in distributing V_{s30} by sub-census block (**Figure 5**).

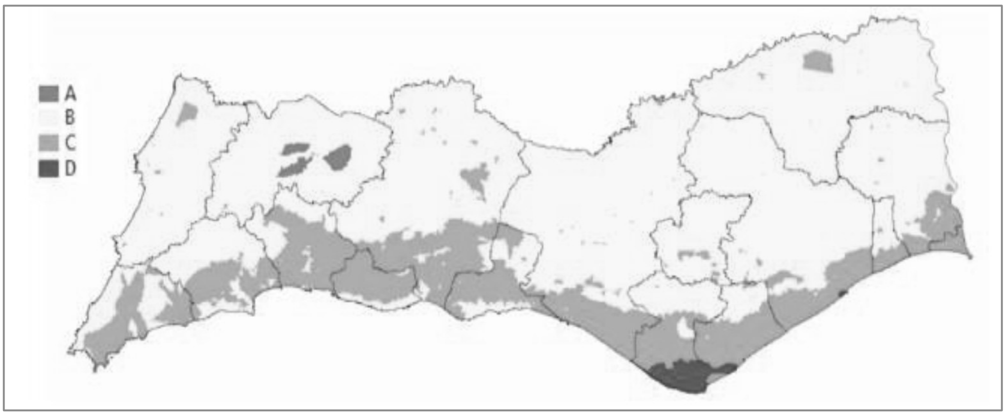

Figure 5. EC8 soil class map - topographic V_{s30} as source

- ✓ <u>Geological analysis - V_{s30}-geology (as a proxy for A_{k3}).</u> This proxy is based on a series of maps established on attempted correlations between geological units and the shear wave velocity to estimate the average *Vs30*. (Wills and Clahan, 2006) proposed a correlation between simplified geologic units and matching V_{s30} values. (Narciso *et al.*, 2013) and [42] adapted that procedure using geologic survey maps and related field data. Using the latter method, a GIS distributed V_{s30} by sub-census block Figure 6).

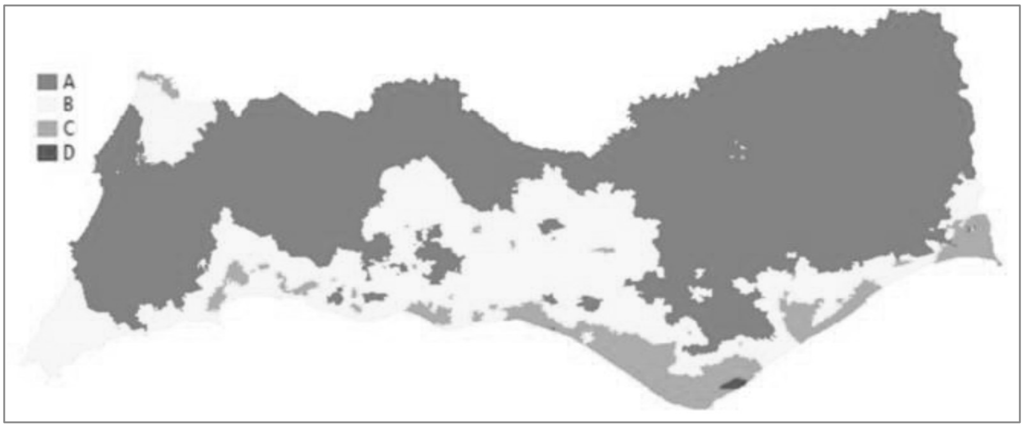

Figure 6. EC8 soil class map - geologic V_{s30} as source

3.1.1 Statistics for each V_{s30} *source*

The analysis of the data consisted of descriptive statistical tests. Table 1 describes the average, median, standard deviation, minimum and maximum for all the V_{s30} with different data source.

Table 1. Descriptive Statistics for all V_{s30} sources

	V_{s30}-field-data	Proxy V_{s30}-slope	Proxy V_{s30}-geology
Average	830	358	684
Median	818	348	689
Standard Deviation	153	68	49
Minimum	120	184	253
Maximum	1156	783	1527

3.1.2 Inferential analysis for V_{s30}

In the inferential analysis, a Pearson's Linear correlation coefficient (Pearson, 1895), a Correlation Coefficient Significance and a scatter plot have been used.

- ✓ **Pearson's Linear correlation coefficient (r)**

This coefficient is a measure of the strength of a linear association between variables. This has a value between +1 and -1, where +1 is a full positive linear correlation, 0 is a non-linear correlation and -1 is a full negative linear correlation. Table 2 shows that the best correlation is between the V_{s30}-field-data and the V_{s30}-geology profile with r = 0.927. This correlation is better than the one existing between the V_{s30}-slope and the V_{s30}-field-data (0.596).

Table 2. Pearson correlation coefficient (*r*) matrix for the V_{s30}.

	V_{s30}-field-data	Proxy V_{s30}-slope	Proxy V_{s30}-geology
V_{s30}-field-data	1.000	0.596	0.927
Proxy V_{s30}-slope	--	1.000	0.701
Proxy V_{s30}-geology	--	--	1.000

However the approach to estimate the V_{s30}-slope can be misleading for this particular case (Wald and Allen, 2007). This assumption is supported by the recommendation to include direct measurements of the seismic velocities for site characterisation (Ahdi *et al.*, 2017).

✓ **Correlation Coefficient Hypothesis Test**

A significance test has been undertaken to derive a *P*-value for the correlation coefficient (r=0.929), with a statistical hypothesis tested as proposed by [83]. The *P*-value obtained for the significance test has been P<0.022, signalling a significant positive correlation between V_{s30}-field-data and proxy V_{s30}-geology.

✓ **Scatter Plot**

When investigating an association it is important to review the result of the significance test along with the value of the correlation coefficient by performing a scatter plot of the two variables. In this framework, Figure 7 plots the relationship between V_{s30} field data and both V_{s30} proxies.

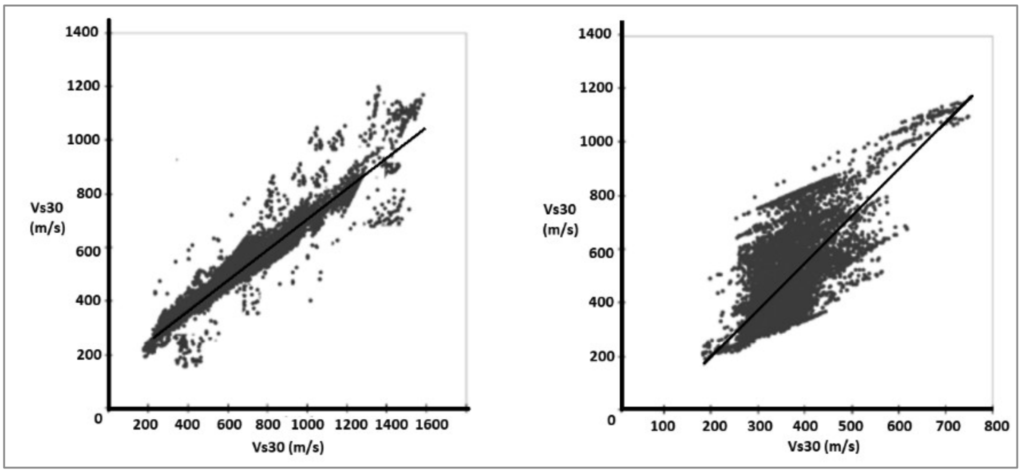

Figure 7. Relation between V_{s30}-field-data and a) V_{s30}-geological (left); b) V_{s30}-slope (right).

By analysing the previous figure, an irregular dispersion can be observed for the proxy V_{s30} slope when compared with the V_{s30} field data. The latter can be observed in a broad distribution of the plot on the right. On the left plot V_{s30} distributions seem to follow a linear behaviour, feasibly showing a better fit between the V_{s30} field data and the proxy V_{s30} geology.

3.2 Determination of the amplification factors (A_{k1}/A_{k2}/A_{k3}) from V_{s30} empirical equations

In order to calculate the amplification factors, the authors selected simple empirical formulas based on Vs30, some of them quite old but still in use by many applications related with design and construction project, where soil amplification is usually calculated from practical and direct formulas (Senkaya *et al.*, 2016). For this objective, the V_{s30} has been inferred from the combination of (Joyner and Fumal, 1984), (Midorikawa, 1987), (Borcherdt *et al.*, 1991) and (Stewart *et al.*, 2005) models. The expected value (A_k) for a one-second period has been considered.

$$A_k = -0.51 \times \log\left(\frac{V_{s30}}{V_o}\right)$$ **(5)** (Joyner and Fumal, 1984)

where V_0 is the reference shear velocity (for 1s period corresponds V_0 = 1580 m/s)

$$A_k = 68 \times V_{s30}{}^{-0.6}$$ **(6)** (Midorikawa, 1987)

$$A_k = \frac{598}{V_{s30}}\ (strong\ motion);\ A_k = \frac{701}{V_{s30}}\ (weak\ motion)$$ **(7)** (Borcherdt *et al.*, 1991)

$$A_k = e^{(a_1 + b_1 \ln(pHAr))}$$ **(8)** (Stewart *et al.*, 2005)

where a_1, b_1 are unidimensional parameters and *pHAr* refers to the reference peak horizontal acceleration for rock (for 1s period, *pHAr = 0.1g)*.

The results of equations (5) to (8) have been weighted using a logic tree approach (Annaka *et al.*, 2007), to address the epistemic uncertainties in ground-motion characterization (Figure 8). Table 3 shows the main characteristics of each model.

Table 3. Characteristics of the empirical models.

Model	Data source	M_w interval
(Joyner and Fumal, 1984)	California	6.4
(Midorikawa, 1987)	Japan	6.7
(Borcherdt *et al.*, 1991)	California	6.9
(Stewart *et al.*, 2005)	Worldwide	4.4 – 7.4

The analysis of Equations (5) to (8) and the field data source has led to a weighted value for each model. This is understood as the relative likelihood of the experimenter´s concern relating each model, as described in Figure 3. The findings of (Midorikawa, 1987) stemmed from data collected from Japanese earthquakes. The data used by (Borcherdt *et al.*, 1991) is from the Loma Prieta event and from records of the 1906 San Francisco earthquake. The data by (Joyner and Fumal, 1984) were essentially collected from the 1979 Imperial Valley event – Baja California. Only (Stewart *et al.*, 2005) used data collected worldwide. Due to the geographic distribution of the datasets and the magnitude scope of each model, the authors approach was to combined the expressions with equal weights, as the reference amplification parameter (Ak) was estimated as the mean of the four empirical formulas results.

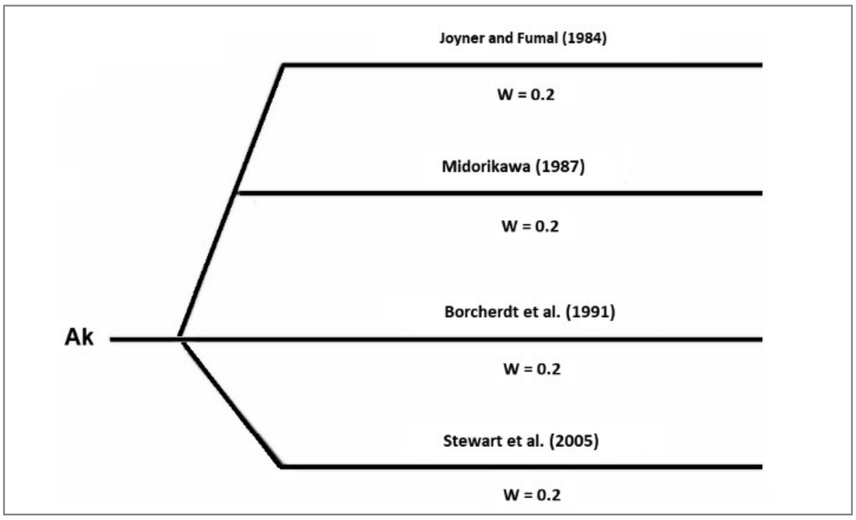

Figure 8. Logic tree used for the estimation of the empirical amplification factors (A_{k1} / A_{k2}).

The analysis of Table shows that most of the equations chosen use local/regional data for seismic active regions. This problem is cumulative with the maximum magnitude, limiting this variable to M_w7,4. The constraint exists due to the inexistence of empirical equations for SW Iberian amplifications. This is because of the limited observations of seismic motion, as the last major seismic event felt in this area was the 1969 earthquake (M_s≈7,5) (Fukao, 1973). This circumstance is a work limitation for every analysis in this specific region, as it is capable of introducing a bias on the amplification estimation when applied in moderate seismicity area like Algarve.

3.3 Intensity felt

The ground motion at the bedrock has been estimated using the (Vilanova and Fonseca, 2007) model - Equation (3). The 1856 (Carvalho *et al.*, 2012) and the 1969 (Grandin *et al.*, 2007) events were computed. The bedrock ground motion values (in PGA) have been converted into peak 5% damped PSA (1Hz) using Equation (4). Regarding the site effects, the soil amplification factors (A_k) have been taken as the ratio of the spectral acceleration at the surface and the spectral acceleration at the bedrock. So, the spectral acceleration at the bedrock – obtained from Equation (4)- has been multiplied by the amplification factor and the final value for the spectral acceleration observed in each census track has been computed:

$$Spectral\ acceleration_{(bedrock)} \times A_k = Spectral\ acceleration_{(surface)} \quad (9)$$

The (Atkinson and Kaka, 2007) conversion equation has been used to transform the PSA, for a 1s period, into MMI:

$$MMI = 0.57 + 2.95\ \log PSA\ (\log\ PSA \geq 1.4g) \quad (10)$$

$$MMI = 3.23 + 1.18\ \log PSA\ (\log\ PSA < 1.4\ g) \quad (11)$$

The EMS98 [74] based vulnerability relationships and the buildings fragility curves suggested by [73] have been used. The MMI-values obtained have been employed to infer the potential damage to the Algarve stock building as proposed by [39] through the vulnerability index (V_i). The damage to population (deaths, injuries, homeless) has been estimated using the method developed by [75], which is based on the assessment of the number of buildings in different states of damage.

4. Application

A loss assessment has been made considering the three amplification factors for the 1856 and 1969 events. First, the output generated by the different amplifications factors has been statistically analysed. Later, the intensities felt have been studied by means of isoseismal maps. Finally, the damage in buildings and human losses has been evaluated.

4.1 Amplification factors

The amplification factors (A_k) calculated have been analysed by means of statistical analysis. Basic statistics for each variable (A_{k1} to A_{k3}) can be observed in Table 2.

Table 2. Linear statistics for each amplification factor.

	A_{k1}	A_{k2}	A_{k3}
Maximum	2.373	2.110	2.083
Average	1.318	1.578	1.410
Median	1.360	1.565	1.450
Minimum	0.796	1.092	0.877
Standard Deviation	0.310	0.135	0.242

The histogram for each amplification factor is shown in Figure 9.

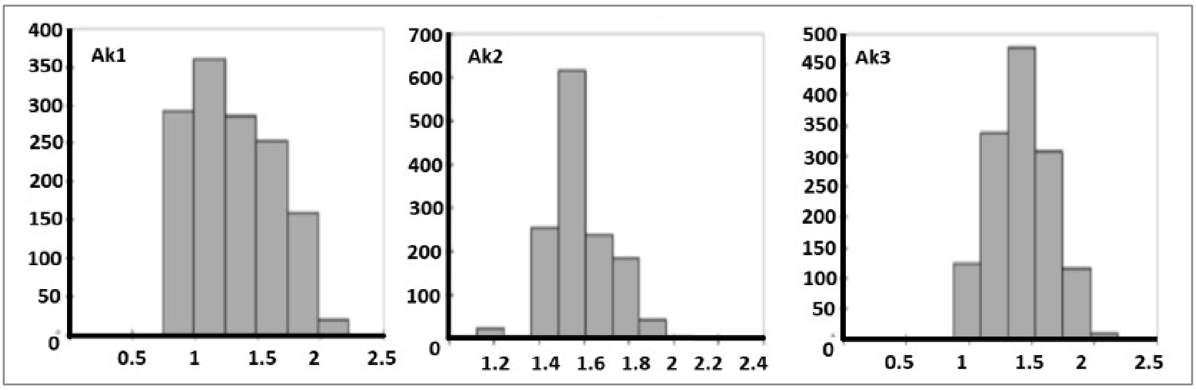

Figure 9. Histogram for the amplification factors (A_{k1} to A_{k3}).

The best matches among the different amplifications computed are those between the V_{s30}-based (bigger between A_{k2} and A_{k3} and smaller between those and A_{k1}). Also, the Pearson correlation coefficient **–***r*- (Pearson, 1895) has been used to analyse the amplification factors and similar conclusions have been drawn (Table 3).

Table 3. Pearson correlation coefficient (*r*) matrix between the amplification factors.

	A_{k1}	A_{k2}	A_{k3}
A_{k1} (V_{s30}-field-data)	1.000	0.613	0.937
A_{k2} (V_{s30}-slope)	--	1.000	0.721
A_{k3} (V_{s30}-geology)	--	--	1.000

From Table 3, it can be observed that the best correlation is between A_{k1} and A_{k3} (r = 0.937). This is a strong correlation, possibly justified by the use of the same source although with different methods. The correlation between A_{k2} and A_{k3} is moderate to strong (r = 0.721).

4.2 Ground motion

The output data has been used to build an isoseismal map for each event. However their reliability has to be assessed individually with respect to the data applied (Schenková *et al.*, 2007). In Figure 10, it can be observed that there are similitudes in the intensity intervals between the amplification factors used for the same event. For the 1856 earthquake, the isoseismal shapes are similar with minor differences for the field intensity at the epicentre. The intensity ranges between 5≤MMI≥8. These intensities are consistent with the macroseismic intensity felt in the 1856 earthquake coeval records (Martínez-Solares and Mezcua Rodríguez, 2002).

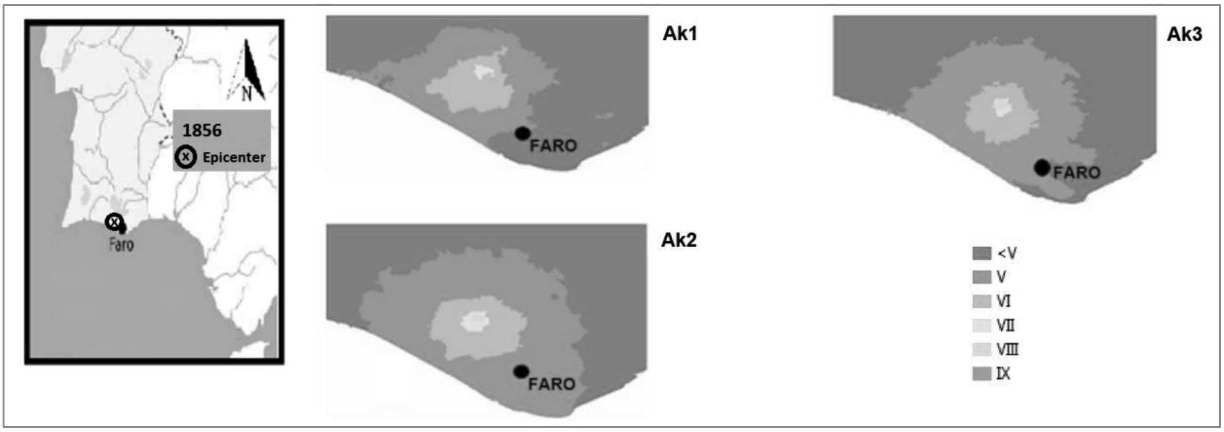

Figure 10. Isoseismal maps for the 1856 earthquake using A_{k1}-A_{k3}.

The existing instrumental records for the 1969 earthquake enabled a more detailed revision. An analysis of this event can be read in (Grandin *et al.*, 2007). A related isoseismal map based in seismic observations is illustrated in Figure 11, where intensities reach a maximum of VII-VIII.

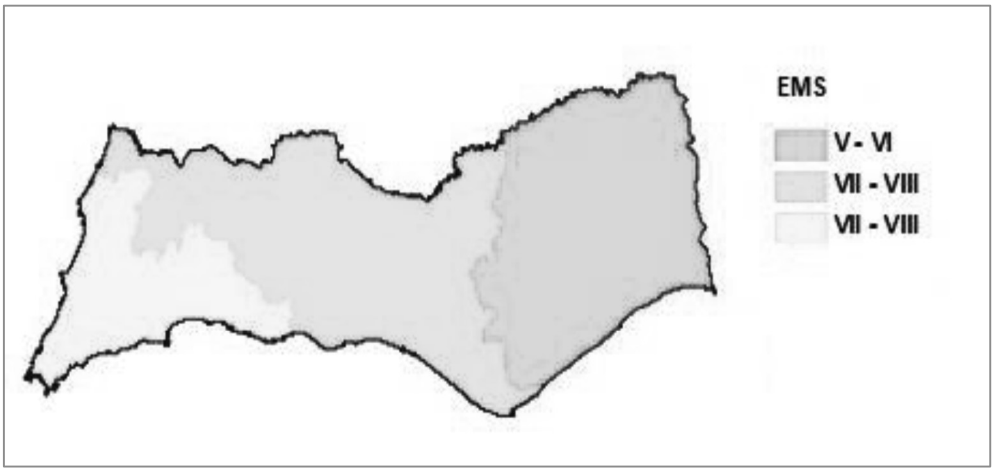

Figure 11. Isoseismal map for the 1969 earthquake as proposed by (Sousa, 2006)

The same value range is predicted by this work as depicted in Figure 12. It can be observed that the shape of the isoseismal areas is similar although with dissimilarities between A_{k1}-A_{k3}, and more relevant for MMI=VI between A_{k1} and the other amplification factors.

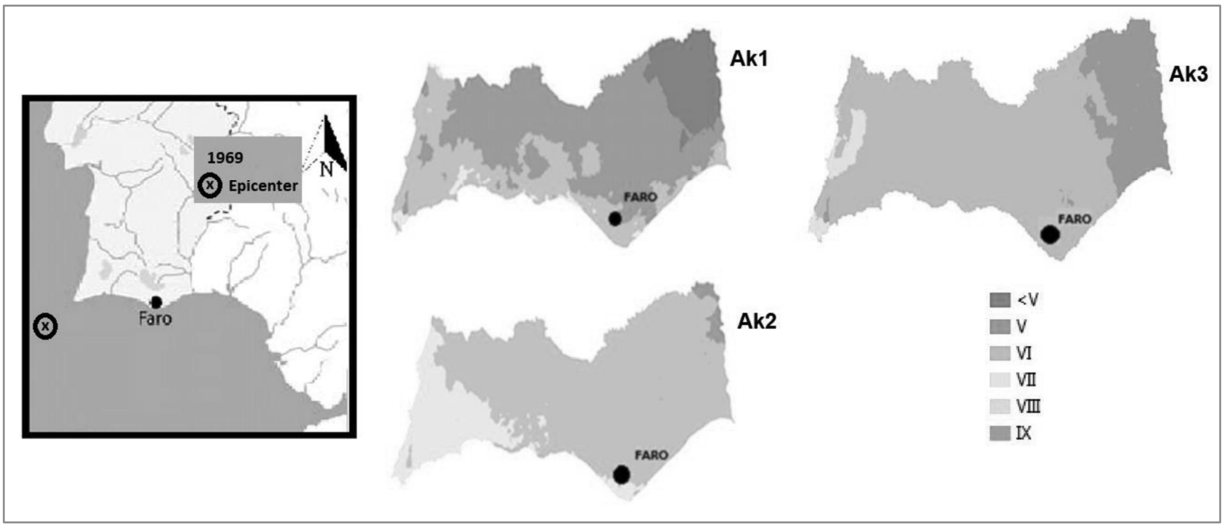

Figure 12. Isoseismal maps for the 1969 earthquake using A_{k1}-A_{k3}

The MMI variable is of mathematical discrete nature, therefore to work with quantitative data, PGA must be calculated. To do so, PSA values obtained from Equation (9) have been converted into PGA using Equation (4). This allows an enhanced statistical analysis due to the use of what is now a continuous variable. In this framework a Pearson correlation for each ground motion dataset has been made assuming a normal behaviour for the tested sample. Considering all the aforementioned, Tables 6 and 7 detail the ground motion in PGA at the surface level (bedrock + site effects) for each scenario.

Table 4. Pearson correlation (*r*) matrix between the PGA values for the 1856 earthquake.

	PGA A_{k1}	PGA A_{k2}	PGA A_{k3}
PGA A_{k1}	1.000	0.689	0.575
PGA A_{k2}	--	1.000	0.720
PGA A_{k3}	--	--	1.000

Table 5. Pearson correlation (*r*) matrix between the PGA values for the 1969 earthquake.

	PGA A_{k1}	PGA A_{k2}	PGA A_{k3}
PGA A_{k1}	1.000	0.622	0.563
PGA A_{k2}	--	1.000	0.922
PGA A_{k3}	--	--	1.000

The *r* has a value of 0.720 (1856 event) – 0.922 (1969 event), which is a moderate to strong positive association between A_{k2} (V_{s30}-slope) and A_{k3} (V_{s30}-geology). The relation between A_{k1} (V_{s30}-real-data) and A_{k2} (V_{s30}-slope) is moderate with an r between 0.689 (1856) and 0.622 (1969). With the statistics obtained is reasonably to conclude that the strongest relation is between A_{k2} (V_{s30}-slope) and A_{k3} (V_{s30}-geology).

4.3 Building damage and human losses

The seismic risk can be estimated as the combination of the intensity of a phenomenon and the exposure of vulnerable elements to this occurrence (Fazendeiro Sá *et al.*, 2016). The seismic risk is determined as the combination of hazard - the earthquake ground motion – perceived in each building site and the macroseismic vulnerability of each dwelling typology using the EMS98 (Grünthal, 1998). The seismic risk is expressed via the losses degree. The losses for each scenario are conveyed in deaths, victims with injuries, homeless people, and severe damage buildings or collapsed ones.

First, to calculate the building damage, the (Giovinazzi and Lagomarsino, 2004) vulnerability index (V_i) method has been used to calculate the number of buildings with different degrees of damage. With this method, the fragility curve of each building indicates the likelihood of suffering some degree of damage (from D1 to D5 of the EMS98 damage scale (Grünthal, 1998)) depending on the macroseismic intensity (I-XIII) produced by an earthquake. The most relevant degrees of damage are D4 (severe damage) and D5 (collapse) as they produce unusable buildings.

Regarding the estimation of the human losses, (Coburn *et al.*, 1992) proposed a model to estimate the number of victims. This model considers the type of construction, the building population, the occupation at the time of the occurrence of the earthquake, the number of occupants trapped in the debris, the distribution of lesions and the evolution of the mortality of survivors who have been trapped. The "fatality rate", the ratio between the number of deaths and the number of occupants within the damaged buildings, is set to estimate the number of victims (Coburn *et al.*, 1992). The latter is determined considering the number of pre-collapsed and collapsed buildings and their lethality factor (essentially D4 and D5). For the 1856 and the 1969 earthquakes, the losses are listed in Table 6.

Table 6. Human losses and building damage for the 1856 and the 1969 earthquakes.

Earthquake	1856			1969		
Amplification factor used	A_{k1}	A_{k2}	A_{k3}	A_{k1}	A_{k2}	A_{k3}
Deaths	1	4	2	63	127	74
Injured	5	14	11	198	376	207
Buildings unusable (D4+D5)	0	4	8	70	264	63
Homeless	0	6	19	63	127	105

Table 9 shows the same output as a percentage of the total Algarve population and building stock considering the 2011 census.

Table 7. Human losses and building damage as percentage of existing buildings and population.

Scenario	*1856*			*1969*		
Amplification factors used	A_{k1}	A_{k2}	A_{k3}	A_{k1}	A_{k2}	A_{k3}
Losses (deaths + injured)	0.001%	0.001%	0.001%	0.063%	0.033%	0.041%
Buildings damaged (D4/D5)	0.000%	0.004%	0.004%	0.035%	0.133%	0.032%

It can be observed that the inter-earthquake differences are minimal regarding the damage building 0.004% for the 1856 event and 0.135% for the 1969 event) and the human losses (0.001% and 0.063%, respectively). These inaccuracies can be considered acceptable, as shown in similar analyses where different loss assessment procedures were applied (King and Rojahn, 1996), (Spence *et al.*, 2008) and (Spence and So, 2009).

5. Discussion

In this research, 1D soil amplification using different sources for V_{s30} is compared. First, some theoretical backgrounds on synthetic models are described. Later, real sub-surface conditions are presented. The results of the different soil amplification values have been introduced into the hazard model of a regional seismic risk simulator. A vulnerability model has been used to analyse different risk outputs. In this framework, the averaged shear-wave velocity to 30 m (V_{s30}) is a significant parameter for many GMPEs and building codes. Nevertheless, in some cases V_s profiles do not extend up to 30 m or such data is unavailable, which forces estimating the V_{s30} by proxy.

Because of variations in geologic conditions, a proxy-based estimation of V_{s30} is best assumed at a local level, as apparently similar conditions in different regions can have dissimilar velocity structures (Scasserra *et al.*, 2009). (Castellaro *et al.*, 2008) and (Lemoine *et al.*, 2012) question the use of V_{s30} as a valid proxy for seismic amplification, especially without site-specific conditions. However, hazard and risk maps are dependent on the V_{s30} due to the inexistence of alternatives (Wald *et al.*, 2011). (Wald and Allen, 2007) proposed using the V_{s30} as a site classification for potential amplifications in regions without V_{s30} real data. Nevertheless, the use of proxies based on the topographic slope shows somewhat unbiased distributions of the logarithm of V_{s30} (Narciso *et al.*, 2013). Contrariwise, in SW Iberia, the use of geologic V_{s30} proxy as proposed by (Narciso *et al.*, 2013), [32] and [42] seems to insure a better adjustment on emulate real data.

This research considers the V_{s30} from a practical point of view and comparatively analyses the usage of V_{s30} real data, V_{s30} slope and a geological-based principle for estimating the potential consequences of an earthquake. In that context, output data from assessment losses indicate that the degree of correlation between different V_{s30} sources is unbiased to the estimation of those losses.

Finally, the authors wish to highlight the limitations of using V_{s30} values at a local scale without the necessary adjustment to the local soil conditions. Even so, it is expected that the V_{s30} as an amplification proxy will continue to be used due to its simplicity and inexpensiveness. For that reason, in this research, the use of the V_{s30} has been upheld and the results related have been analysed, considering a regional or even less detailed scale framework.

6. Conclusions

In this research, two scenarios have been considered: the inland 1856 earthquake -M_w5.5- (Carvalho *et al.*, 2012) and the onshore 1969 Gorringe earthquake -M_w7.8- (Grandin *et al.*, 2007). The premises proposed have been tested and the results show the following conclusions:

1. The three amplifications factors A_{k1} (achieved using V_{s30}-field-data), A_{k2} (using the V_{s30}-slope) and A_{k3} (using the V_{s30}-geology) have shown a moderate to good correlation between each other. The best correlation has been achieved between A_{k1} and A_{k3}. Therefore, for this case, the V_{s30} based on (Wills and Clahan, 2006) proposal is the best proxy for actual soil values.
2. Using an EC8 classification, three sources of V_{s30} generated maps with dissimilar shapes an aspect particularly perceived in inland areas (Figures 4 to 6), reflecting the existence of differentiated site effects. However, final records for loss assessment don´t prove the existence of much difference between V_{s30} scenarios.
3. This unpredicted circumstance can be explained by the fact that inland areas - where major differences between EC8 maps are perceived - are characterized by a smaller population density. This specifics result in a low risk level for inland areas - large hazard vs. low exposure - thus diminishing the performance of the losses output. This condition is potentially enhanced by the aggregation of the loss assessment data, presented only for Algarve as a macro region (Tables 8 and 9).

4. The values for the ground motion at the surface level - as peak ground acceleration - show a correlation factor marginally superior for the 1969 earthquake, which is an onshore event with a distant epicentre.
5. The seismic wave period selected for this research has been 1s. The wave period is important as a physical phenomenon and is a variable necessary for estimate amplification in Equations 5 and 8. A scenario of lower (<1s) and bigger periods (up to 30s) must be analysed in future works, due to the existence of building stock with different periods, circumstance determined largely by the presence of differentiated stories number.
6. The seismic losses are similar when using different amplification factors for both scenarios. Moreover, these values are consistent with the output offered by the Portuguese Civil Protection Seismic Risk Simulator for the same scenario.
7. In this research, in terms of seismic risk assessment, considering the seismic losses, the differences reported between the soil amplification factors have not been transferred to the final results, establishing that a correlation between different V_{s30} sources seems unbiased to the estimation of seismic losses. That is, the losses output show that for the trial conditions, the difference between calculating the site effects with different $\mathbf{V}_{s30}$ sources are minor.
8. In this framework, and in the absence of real V_{s30} values, the authors recommend using the (Wills and Clahan, 2006) procedure instead of the method proposed by (Wald and Allen, 2007).
9. In the above framework, the authors credit that for SW Iberia a simulator for a regional scale, which characterises the site effects by proxy V_{s30}-geology works properly.
10. For emergency planning purposes the results achieved and the conclusions inferred show that using the solution V_{s30} as amplification proxy, and specifically the V_{s30}-geology solution, an accurate result for loss estimation can be generated.

7. Data and resources

V_{s30} real data used in this work has been obtained by field work performed in the framework of ERSTA project and has been graciousness shared by the *Autoridade Nacional de Proteção Civil*. The DEM used to obtain the gradients is a 30-arcsec-resolution. This includes data from the Shuttle Radar Topography

Mission - flown in Feb 2000 - and data from the U.S. Geological Survey (USGS) - GTOPO30 set (https://lta.cr.usgs.gov; accessed Dec 2017). The geology discussed is based on data from the National Laboratory for Geology and Energy (LNEG) - available in the OneGeology project, http://www.onegeology.org, accessed Nov 2017. All computation have been made in the Microsoft Excel environment enriched with VBA routines. ESRI ArcGis 10.1 has been used for the map analysis.

8. Acknowledgements

The authors would like to acknowledge their gratitude to *Autoridade Nacional de Proteção Civil* for their graciousness in sharing information and data related with this research. This research has been financed by the internationalisation aid of the University Institute of Architecture and Construction Sciences with the Own Plan for Research and Transfer of the University of Seville.

9. Computer Code Availability

The simulator software cited in this work was named "SIRCO". It´s a package coded in Visual Basic for Applications (VBA), an event-driven programming language that uses the Visual Basic Runtime Library. The code requires a computer with 2 Gb RAM and a 1.5 GHz processor in a MAC OS or Microsoft Windows environment as minimum requirements. A Microsoft Excel installation, including the VBA7 package, is also mandatory. For more detailed information about the simulator software itself please refer to (Sá *et al.*, 2016).

The programming code is available by using the link: https://github.com/shedore/sim.git

10. References

Ahdi, S.K., Stewart, J.P., Kwak, D.Y., Al., E., 2017. Proxy-Based V S30 Prediction in Alaska Accounting for Limited Regional Data. 3rd Int. Conf. Perform. Based Des.

Aki, K., Richards, P.G., 1981. Quantitative Seismology: Theory and Methods. Geol. J. 16, 1–900. https://doi.org/10.1002/gj.3350160110

Amaro-Mellado, J.L., Morales-Esteban, A., Asencio-Cortés, G., Martínez-Álvarez, F., 2017a. Comparing seismic parameters for different source zone models in the Iberian Peninsula. Tectonophysics. https://doi.org/10.1016/j.tecto.2017.08.032

Amaro-Mellado, J.L., Morales-Esteban, A., Martínez-Álvarez, F., 2017b. Mapping of seismic parameters of the Iberian Peninsula by means of a geographic information system. Cent. Eur. J. Oper. Res. https://doi.org/10.1007/s10100-017-0506-7

Ambraseys, N.N., Simpson, K.A., Bommer, J.J., 1996. Prediction of Horizontal Response Spectra in Europe. Earthq. Eng. Struct. Dyn. 25, 371–400. https://doi.org/10.1002/(SICI)1096-9845(199604)25:4<371::AID-EQE550>3.0.CO;2-A

Annaka, T., Satake, K., Sakakiyama, T., Yanagisawa, K., Shuto, N., 2007. Logic-tree Approach for Probabilistic Tsunami Hazard Analysis and its Applications to the Japanese Coasts. Tsunami its hazard Indian Pacific Ocean. 577–592.

Antunes, M.T., Legoinha, P., Proença, C.P., Pais, J., 2000. High resolution stratigraphy and miocene facies correlation in Lisbon and Setubal Peninsula (Lower Tagus basin, Portugal). 1º Congr. sobre Cenozóico Port. 14, 183–190.

Antunes, M.T., Pais, J., 1993. The Neogene of Portugal. Proc. 1st R.C.A.N.S. Congr. 12, 7–22.

Atkinson, G.M., Boore, D.M., 1997. Stochastic Point-Source Modeling of Ground Motions in the Cascadia Region. Seismol. Res. Lett. 68, 74–85. https://doi.org/10.1785/gssrl.68.1.74

Atkinson, G.M., Kaka, S.L.I., 2007. Relationships between felt intensity and instrumental ground motion in the Central United States and California. Bull. Seismol. Soc. Am. 97, 497–510. https://doi.org/10.1785/0120060154

Autoridade Nacional de Protecção Civil (ANPC), 2010. Estudo do Risco Sísmico e de Tsunamis do Algarve. Lisbon. (in Portuguese)

Bisch, P. 2018. Eurocode 8. Evolution or Revolution?. In European Conference on Earthquake Engineering Thessaloniki, Greece (pp. 639-660). Springer, Cham.

Bommer, J.J., Douglas, J., Scherbaum, F., Cotton, F., Bungum, H., Fah, D., 2010. On the Selection of Ground-Motion Prediction Equations for Seismic Hazard Analysis. Seismol. Res. Lett. 81, 783–793. https://doi.org/10.1785/gssrl.81.5.783

Boore, D.M., 1983. Stochastic simulation of high-frequency ground motions based on seismological models of the radiated spectra. Bull. Seismol. Soc. Am. 73, 1865–1894.

Boore, D.M., Atkinson, G.M., 1987. Stochastic Prediction of Ground Motion and Spectral Response Parameters At Hard-Rock Sites in Eastern North America. Bull. Seismol. Soc. Am. 77, 440–467. https://doi.org/10.1017/CBO9781107415324.004

Boore, D.M., Joyner, W.B., Fumal, T.E., 1993. Estimation of response spectra and peak accelerations from western North American earthquakes: an interim report. USGS Open-File Rep. 72pp.

Booth, E., 2007. The estimation of peak ground-motion parameters from spectral ordinates. J. Earthq. Eng. 11, 13–32. https://doi.org/10.1080/13632460601123156

Borcherdt, R., Wentworth, C.M., Janssen, A., Fumal, T., Gibbs, J., 1991. Methodology for predictive GIS mapping of special study zones for strong ground shaking in the San Francisco Bay region, California, in: 4th Int. Conf. Seismic Zonation. pp. 545–552.

Borges, J.F., Bezzeghoud, M., Caldeira, B., Carvalho, J., 2015. Ground-Motion Simulation in Lower Tagus Valley Basin. Pure Appl. Geophys. 172, 2411–2420. https://doi.org/10.1007/s00024-015-1060-7

Brachert, T.C., Forst, M.H., Pais, J.J., Legoinha, P., Reijmer, J.J.G., 2003. Lowstand carbonates, highstand sandstones? Sediment. Geol. 155, 1–12. https://doi.org/10.1016/S0037-0738(02)00329-9

Carvalho, J., Dias, R., Pinto, C., Leote, J., Mendes-Victor, L., 2008. A Soil Classification For Seismic Hazard Assessment and Mitigation Of The Algarve, in: 14th World Conference on Earthquake Engineering (14WCEE). Beijing, China, pp. 1–8.

Carvalho, J., Matias, H., Rabeh, T., Menezes, P.T.L., Barbosa, V.C.F., Dias, R., Carrilho, F., 2012. Connecting onshore structures in the Algarve with the southern Portuguese continental margin: The Carcavai fault zone. Tectonophysics 570–571, 151–162. https://doi.org/10.1016/j.tecto.2012.08.011

Castellaro, S., Mulargia, F., & Rossi, P. L., 2008. VS30: Proxy for seismic amplification?. Seismological Research Letters, 79(4), 540-543.

Chester, D.K., 2001. The 1755 Lisbon earthquake. Prog. Phys. Geogr. 25, 363–383. https://doi.org/10.1191/030913301680193823

Coburn, A., Spence, R., Pomonis, A., 1992. Factors determining human casualty levels in earthquakes:

Mortality prediction in building collapse, in: X World Conference on Earthquake Engineering. Madrid, Spain, pp. 19–24.

Crespo, M.J., Martínez, F., Martí, J., 2013. Seismic hazard of the Iberian Peninsula: Evaluation with kernel functions. Nat. Hazards Earth Syst. Sci. 14, 3763–3811. https://doi.org/10.5194/nhess-14-1309-2014

Cunha, P.P., Pais, J., Legoinha, P., 2009. Geologic evolution of the Portugal mainland during the Cenozoic - alluvial and marine sedimentation at a passive continental margin (W Iberia), in: 6º Simposio Sobre El Margen Ibérico Atlántico MIA09. Oviedo, pp. 1–10.

Dabrio, C.J., Armenteros, I., Civis, J., Pais, J., 2008. Facies changes and paleogeographical implications in the Serravallian of the Lagos-Portimão Formation (Praia da Rocha , southern Portugal). Geo-Temas 10, 131–134.

Derras, B., Bard, P. Y., & Cotton, F., 2016. Site-condition proxies, ground motion variability, and data-driven GMPEs: Insights from the NGA-West2 and RESORCE data sets. *Earthquake spectra*, *32*(4), 2027-2056.

Dias, R., Cabral, J., 2002. Neotectónica da região do Algarve, in: Comun. Inst. Geol. e Mineiro. pp. 193–208. (in Portuguese)

EN1998-1, 2004. Eurocode 8: Design of structures for earthquake resistance. Part 1: General rules, seismic actions and rules for buildings.

Eurostat (2019). Eurostat database [online].[cit. 2019-01-10]. *http://ec. europa. eu/eurostat/data/database*.

Fazendeiro Sá, L., Morales-Esteban, A., Durand Neyra, P., 2016. A seismic risk simulator for Iberia. Bull. Seismol. Soc. Am. 106. https://doi.org/10.1785/0120150195

FEMA, 2015. NEHRP Recommended Seismic Provisions for New Buildings and Other Structures, 2015th ed. Washington, D.C.

Field, E.H., Jacob, K.H., 1995. A comparison and test of various site-response estimation techniques, including three that are not reference-site dependent. Bull. Seismol. Soc. Am. 85, 1127–1143.

Fukao, Y., 1973. Thrust faulting at a lithospheric plate boundary. The Portugal earthquake of 1969. Earth Planet. Sci. Lett. 18, 205–216.

García-Jerez, A., Luzón, F., Navarro, M., 2008. An alternative method for calculation of Rayleigh and Love wave phase velocities by using three-component records on a single circular array without a central station. Geophys. J. Int. 173, 844–858. https://doi.org/10.1111/j.1365-246X.2008.03756.x

Gaudio, V., Pierri, P., Venisti, N., 2019. Site classification of Italian accelerometric stations from cluster analysis of residuals of peak ground motion data regressions. Science of The Total Environment, 681, 39-55.

Geirnaert, W., van Beers, P.H., De Vries, J.J., Hoogeven, H., 1982. A geoelectric survey of the Miocene aquifer between Quarteira and Olhão, Algarve, Portugal, in: Lisboa, D. de G. da F. de C. de (Ed.), III Semana de Hidrogeologia.

Giovinazzi, S., Lagomarsino, S., 2004. A macroseismic method for the vulnerability assessment of buildings, in: 13th World Conference on Earthquake Engineering. Vancouver, B.C., Canada.

Grandin, R., Borges, J.F., Bezzeghoud, M., Caldeira, B., Carrilho, F., 2007. Simulations of strong ground motion in SW Iberia for the 1969 February 28 (M_s = 8.0) and the 1755 November 1 ($M \sim 8.5$) earthquakes - II. Strong ground motion simulations. Geophys. J. Int. 171, 807–822. https://doi.org/10.1111/j.1365-246X.2007.03571.x

Grünthal, G., 1998. European Macroseismic Scale 1998. Centre Européen de Géodynamique et de Séismologie, Luxembourg.

Gutscher, M.A., Baptista, M.A., Miranda, J.M., 2006. The Gibraltar Arc seismogenic zone (part 2): Constraints on a shallow east dipping fault plane source for the 1755 Lisbon earthquake provided by seismic data, gravity and thermal modeling. Tectonophysics 426, 153–166. https://doi.org/10.1016/j.tecto.2006.02.024

Joyner, W.B., Fumal, T.E., 1984. Use of Measured Shear-Wave Velocity for Predicting Geologic Site Effects on Strong Ground Motion, in: 8th World Conf. on Earthq. Eng. pp. 777–783.

King, S.A., Rojahn, C., 1996. A comparison of earthquake damage and loss estimation methodologies, in: Eleventh World Conference on Earthquake Engineering. Acapulco (Mexico).

Kotha, S. R., Cotton, F., & Bindi, D., 2018. A new approach to site classification: Mixed-effects Ground Motion Prediction Equation with spectral clustering of site amplification functions. *Soil Dynamics and Earthquake Engineering*, *110*, 318-329.

Le Pense, S., Gatmiri, B., Maghoul, P., 2011. Influence of soil properties and geometrical characteristics of sediment-filled valleys on earthquake response spectra. Proc. 8th Int. Conf. Struct. Dyn. EURODYN 130–136.

Lemoine, A., Douglas, J., Cotton, F., 2012. Testing the Applicability of Correlations between Topographic Slope and VS30 for Europe. Bull. Seismol. Soc. Am. 102, 2585–2599. https://doi.org/10.1785/0120110240

Leyva, F., Ramírez, J., 1979. Hoja de Ayamonte (998) del Mapa Geológico de España a E. 1:50.000, 2ª Serie (MAGNA).

Manuppella, G., 1992. Carta geologica da Regiao do Algarve escala 1:100 000. (in Portuguese)

Martínez-Solares, J.M., Mezcua Rodríguez, J., 2002. Catálogo sísmico de la Península Ibérica (880 a.C.-1990), IGN. ed. Madrid, Spain. (in Spanish)

Midorikawa, S., 1987. Prediction of isoseismal map in the Kanto plain due to hypothetical earthquake. J. Struct. Eng. 33B, 43–48.

Moura, D., Boski, T., 1999. Unidades litostratigráficas do Pliocénico e Plistocénico no Algarve. Comun. Inst. Geol. e Min. 85–106. (in Portuguese)

Murayama, Y., Estoque, R.C., 2011. Zonal Analysis : A GIS lecture tutorial.

Narciso, J., Vilanova, S., Carvalho, J., Pinto, C., Lopes, I., Nemser, E., Sousa Oliveira, C., Borges, J., 2013. Site-condition map for Portugal based on Vs30 values and evaluation of the applicability of Vs30 proxies. EGU Gen. Assem. Conf. Abstr. 15, 11223.

Ozcep, T., Ozcep, F., Ozel, O., 2013. VS30, site amplifications and some comparisons: The adapazari (Turkey) case. Phys. Chem. Earth 63, 92–101. https://doi.org/10.1016/j.pce.2013.05.003

Pais, J., Legoinha, P., Elderfield, H., Sousa, L., Estevens, M., 2000. The Neogene of Algarve (Portugal), in: 1º Congreso Sobre Cenozóico de Portugal. pp. 277–288.

Park, D., Hashash, Y.M.A., 2004. Soil damping formulation in nonlinear time domain site response analysis. J. Earthq. Eng. 8, 249–274. https://doi.org/10.1080/13632460409350489

Paz, M., Leigh, W., 2004. International Building Code IBC-2000. Struct. Dyn. 757–781. https://doi.org/10.1007/978-1-4615-0481-8_25

Pearson, K., 1895. Notes on regression and inheritance in the case of two parents, in: Proceedings of the

Royal Society of London (58). Taylor & Francis, pp. 240–242.

Peláez Montilla, J.A., López Casado, C., Henares Romero, J., 2002. Deaggregation in magnitude, distance, and azimuth in the south and west of the Iberian Peninsula. Bull. Seismol. Soc. Am. 92, 2177–2185. https://doi.org/10.1785/0120010295

Pitilakis, K., Riga, E., & Anastasiadis, A., 2013. New code site classification, amplification factors and normalized response spectra based on a worldwide ground-motion database. Bulletin of Earthquake Engineering, 11(4), 925-966.

Pitilakis, K., Riga, E., Anastasiadis, A., & Makra, K., 2015. New elastic spectra, site amplification factors and aggravation factors for complex subsurface geometry towards the improvement of EC8. In 6th international conference on earthquake geotechnical engineering, New Zealand.

Poormirzaee, R., Moghadam, R.H., 2014. Determination of S-Wave structure via Refraction Microtremor Technique in Urban Area: a Case Study. J. Tethys 2, 347–356.

Pruiksma, J.P., 2016. Nonlinear and Equivalent Linear Site response analysis for the Groningen area. TNO report, R10460, Delft, the Netherlands.

Rahman, M. Z., Siddiqua, S., & Kamal, A. M., 2016. Shear wave velocity estimation of the near-surface materials of Chittagong City, Bangladesh for seismic site characterization. *Journal of Applied Geophysics*, *134*, 210-225.

Rodríguez-Marek, A., Bray, J.D., Abrahamson, N.A., 2001. An Empirical Geotechnical Seismic Site Response Procedure. Earthq. Spectra 17, 65–87. https://doi.org/10.1193/1.1586167

Sá, L. F., Morales-Esteban, A., Durand Neyra, P., 2016. A Seismic Risk Simulator for IberiaA Seismic Risk Simulator for Iberia. Bulletin of the Seismological Society of America, 106(3), 1198-1209.

Sá, L., Morales-Esteban, A., Durand Neyra, P., 2018. The 1531 earthquake revisited: loss estimation in a historical perspective. Bull. Earthq. Eng. 1–27. https://doi.org/10.1007/s10518-018-0367-z

Salazar Rincón, A., 2006. Mapa geológico 1/50.000 de Huelva-Los Caños. (in Spanish)

Scasserra, G., Stewart, J.P., Kayen, R.E., Lanzo, G., 2009. Database for earthquake strong motion studies in Italy. J. Earthq. Eng. 13, 852–881. https://doi.org/10.1080/13632460802566997

Schenková, Z., Schenk, V., Kalogeras, I., Pichl, R., Kottnauer, P., Papatsimba, C., Panopoulou, G., 2007. Isoseismal maps drawing by the kriging method. J. Seismol. 11, 121–129.

https://doi.org/10.1007/s10950-006-9023-1

Senkaya, G. V., Karsli, H., Senkaya, M., 2016. Comparison of soil amplification calculations using Vs30 and impedance ratio. In *SEG Technical Program Expanded Abstracts 2016*(pp. 5001-5005). Society of Exploration Geophysicists.

Silva, J., Estevão, J., Martins, C., 2007. Caracterização Geológica e Geotécnica do Algarve - Estudo de Risco Sísmico e de Tsunamis do Algarve. Escola Superior de Tecnologia da Universidade do Algarve. (in Portuguese)

Silva, V., Crowley, H., Varum, H., Pinho, R., 2015. Seismic risk assessment for mainland Portugal. Bull. Earthq. Eng. 13, 429–457. https://doi.org/10.1007/s10518-014-9630-0

Sokolov, V., Loh, C., Wen, K., 2000. Empirical model for estimating Fourier amplitude spectra of ground acceleration in Taiwan region. Earthq. Eng. Struct. Dyn. 29, 339–357. https://doi.org/10.1002/(SICI)1096-9845(200003)29:3<339::AID-EQE908>3.0.CO;2-R

Sousa, M. L., 2006. Risco sísmico em Portugal continental. Tese de Doutoramento da Universidade Técnica de Lisboa, Lisboa. (in Portuguese)

Spence, R., So, E., 2009. Estimating Shaking-Induced Casualties and Building Damage for Global Earthquake Events, National Earthquake Hazards Reduction Program,. Cambridge (England).

Spence, R., So, E., Jenny, S., Castella, H., Ewald, M., Booth, E., 2008. The Global Earthquake Vulnerability Estimation System (GEVES): An approach for earthquake risk assessment for insurance applications. Bull. Earthq. Eng. 6, 463–483. https://doi.org/10.1007/s10518-008-9072-7

Stewart, J.P., Choi, Y., Graves, R.W., 2005. Empirical Characterization of Site Conditions on Strong Ground Motion. University of California, Berkeley.

Toro, G.R., 2002. Modification of the Toro *et al.* (1997) Attenuation equations for large magnitudes and short distances.

Toro, G.R., Abrahamson, N.A., Schneider, J.F., 1997. Model of Strong Ground Motions from Earthquakes in Central and Eastern North America : Best Estimates and Uncertainties 68, 41–57.

Vilanova, S.P., Fonseca, J.F.B.D., 2007. Probabilistic seismic-hazard assessment for Portugal. Bull. Seismol. Soc. Am. 97, 1702–1717. https://doi.org/10.1785/0120050198

Vilanova, S. P., Narciso, J., Carvalho, J. P., Lopes, I., Quinta-Ferreira, M., Pinto, C. C. & Nemser, E. S. 2018. Developing a Geologically Based VS30 Site-Condition Model for Portugal: Methodology and Assessment of the Performance of Proxies Developing a Geologically Based VS30 Site-Condition Model for Portugal. *Bulletin of the Seismological Society of America*, *108*(1), 322-337.

Vilanova, S.P., Fonseca, J., and Oliveira, C.S., 2012. Ground-Motion Models for Seismic-Hazard Assessment in Western Iberia: Constraints from Instrumental Data and Intensity Observations. Bulletin of the Seismological Society of America, 112, 1, 169-184.

Wald, D., Allen, T., 2007. Topographic Slope as a Proxy for Seismic Site Conditions and Amplification. Bull. Seismol. Soc. Am. 97, 1379–1395. https://doi.org/10.1785/0120060267

Wald, D.J., McWhirter, L., Thompson, E.M., Hering, A.S., 2011. A new strategy for developing Vs30 maps, in: 4th IASPEI/IAEE International Symposium. Effects of Surface Geology on Seismic Motion. Santa Barbara, pp. 1–12.

Wald, L.A., Mori, J., 2000. Evaluation of Methods for Estimating Linear Site-Response Amplifications in the Los Angeles Region. Bull. Seismol. Soc. Am. 90, 32–43. https://doi.org/10.1785/0119970170

Wills, C., Clahan, K., 2006. Developing a Map of Geologically Defined Site-Condition Categories for California. Bull. Seismol. Soc. Am. 96, 1483–1501. https://doi.org/10.1785/0120050179